RSC Advances

ROYAL SOCIETY OF CHEMISTRY

www.rsc.org/advances

Controllable Synthesis of Three-Dimensional Branched Gold Nanocrystals Assisted by Cationic Surfactant Poly(diallyldimethylammonium) Chloride in Acidic Aqueous Solution

Haibin Zhang [a],*, Yonggang Lu[a], Hong Liu[a] and Jingzhong Fang[a]

[a] *Lightweight Optics and Advanced Materials Center, The Institute of Optics and Electronics, Chinese Academy of Sciences, Chengdu, 610209, People's Republic of China.*

* Address correspondence to E-mail: zhb@ioe.ac.cn

Abstract: An effective strategy for the controllable synthesis of single crystalline branched gold nanocrystals with three-dimensional hierarchical structure was realized via the reduction of tetrachloroaurate ions ($AuCl_4^-$) assisted by cationic surfactant poly(diallyldimethylammonium) chloride (PDDA) in acidic aqueous solution. The as-prepared gold nanostructures consisting of main trunks and almost symmetrical side branches presented a [111] plane and grown along the <331> direction. The PDDA and weak reducing agent, ascorbic acid (AA), were indispensable for the formation of these unique gold nanocrystals. The effects of $HAuCl_4$ (or PDDA) concentrations, pH values and reaction temperatures on the morphology of branched gold nanocrystals are discussed in our work. A possible three-staged formation mechanism of initial branched nucleation, subsequent branched nanostructures growth and the final morphology adjustment was proposed on the basis of different reaction times and the corresponding changes in surface plasmon absorption. It is expected that the specific branched gold nanocrystals may find potential applications such as in optoelectronics, surface enhanced Raman scattering (SERS) and surface plasmonics.

1. Introduction

Noble metal nanomaterials, especially gold nanostructures have been the subject of intensive research in recent years, owing to their unique physical and chemical properties and promising applications in catalysis, optoelectronics, sensors, biomedicine and imaging.[1-6] Since their intrinsic properties and relevant applications are highly dependent on morphologies, such as shape and size, great efforts have been devoted to morphology-controlled synthesis of gold nanostructures.[7,8]

To date, various approaches have been reported for synthesizing gold nanocrystals with different morphologies, such as plates,[9] rod-wires,[10] cubes,[11] polyhedra,[12] flowers[13] and branched nanostructures.[14-17] Among them, branched surpermolecular nanostructures attracted much attention with their unique morphology and properties. In general, they have long main trunks and side branches with sharp edges or tips, high surface areas, as well as nanoscale junctions.[18] Additionally, the special anisotropic structures have presented obvious advantages than the common nanoparticles, plates, etc., in many practical applications. Such as in surface enhanced Raman scattering (SERS), [19,20] the branched gold nanostructures have stronger enhancement abilities than nanoparticles or nanospheres.

Therefore, several synthetic approaches have been reported for generating branced or thorn gold nanostructures, including electrochemical,[21] metal replacement,[22] ionic liquid templating,[23] and colloid chemical method.[16, 24-26] In particular, the colloidal chemical method which is a versatile and effective tool for size- and shape-controlled synthesis of branched gold nanostructures has stimulated more interest and received some success in the past few years. For example, Huang and coworkers[25] prepared planar branched gold nanostructures using the complexes of dodecyltrimethylammonium bromide and β-cyclodextrin. Similarly, symmetrical branched nanostructures were obtained in decane-1,10-bis(methylpyrrolidinium bromide) aqueous solution.[26] In these synthesis, surfactants or addictives play an extremely important role by adsorbing on different crystallographic planes and changing the order of the surface free energies, and then directly influence their relative growth rates.[3] Although more and more branched gold nanostructures were gradually realized by using specific surfactants and auxiliary conditions, there are rare reports on three-dimensional crystal growth to generate hierarchical branched architectures, especially for single-crystalline gold nanocrystals.

In this study, we would like to propose a new, facile and effective strategy for the controllable synthesis of single crystalline 3D branched gold nanocrystals with their trunks and side branches grown along <331> directions by the assistance of cationic surfactant PDDA[27,28] in acidic aqueous solution. The effects of the experimental parameters on the morphology of branched gold nanocrystals have been discussed in some detail. The formation process and possible mechanism were investigated on the basis of reaction times and corresponding absorption spectra. Moreover, these unique branched nanostructures with sharp edges and tips possess attractive optical properties, promising their potential applications to optoelectronics, SERS and surface plasmonics.

2. Experimental Section

2.1 Chemicals

Hydrochloroauric acid trihydrate (HAuCl$_4$·3H$_2$O, AR), ascorbic acid (AA, 99.7%), HCl (AR), NaOH (ACS, 97% flakes) were obtained from Aladdin Chemical Regent Co. Ltd (Shanghai, China). Poly(diallyldimethylammonium) chloride (PDDA,

MW=400000-500000 D, 20 wt% in H_2O, $\geq$ 99%) were purchased from Sigma Aldrich. Other reagents were analytical grade and used without further purification. The twice-distilled water was used in all experiments.

2.2 Synthesis of Branched Gold Nanocrystals

In a primary reaction, 0.4 mL portion of 25 mM $HAuCl_4$ aqueous solution, 0.4 mL of PDDA and a given amount of 1 M HCl solution (from 0 to 0.8 mL) were added to 7 mL of pure water in a glass flask. The mixture was stirred with a magnetic blender for 1-2 min at ambient temperature and subsequently heated at 95 $^\circ$C in an oil bath. After 10 min, 2 mL aliquot of 50 mM AA aqueous solution was quickly injected. The color of the gold precursor changed immediately from bright yellowish to reddish brown, indicating the formation of Au nanocrystals. The final solution (pH=3) contains 1 mM, 50 mM, 20 mM, and 10 mM of $[AuCl_4^-]$, PDDA, HCl, AA, respectively. This is later called the standard solution. The whole reaction process was left undisturbed for 30 min, then, the products were collected by centrifugation (12000 rpm, 30 min) and washed repeatedly with water and were resuspended in water or ethanol for characterizations. Further experiments, which were similar to those presented above, were performed under desired conditions.

2.3 Characterization

The products were characterized using X-ray diffraction (XRD, Rigaku D/max-2000 X-ray diffractometer equipped with Cu Kα radiation), field emission scanning electron microscopy (SEM, Hitachi S4800, 5.0 kV), transmission electron microscopy (TEM, FEI Tacnai-G2 F30, 300 kV) together with associated energy-dispersive X-ray (EDX) spectroscopy analysis, and UV-vis absorption measurement (TU-1901 dual beam UV-Vis spectrophotometer).

Specially, the as-prepared sample was pipetted onto a Si wafer or a holey carbon-coated Cu grid for SEM, TEM respectively. Air-dried powder samples were prepared for XRD characterization. UV-vis absorption spectra were obtained by solution analysis in a 1-cm optical length quartz cell.

3. Results and Discussion

3.1 Structural Characterizaion

Figure 1 presents the typical SEM and TEM images of branched gold nanocrystals obtained in the standard solution. As shown in Figure 1a, b, the products are three-dimensional flowerlike nanocrystals with size of ~2 μm, and mainly consisted of aggregated branched structures. The enlarged images (Figure 1c, d) suggest that each nanocrystal presents a hierarchical architecture, which has several main trunks and many side branches reaching in different directions. Clearly, all the trunks

growing from central point and the branches are approximately symmetrical with certain angles, implying that these branched nanocrystals might grow radially from central particles.[25] The XRD patterns (shown in Figure 2d) which exhibit sharp diffraction peaks corresponding to the {111}, {200}, {220}, {311} and {222} planes (Joint Committee on Powder Diffraction Standards (JCPDS) No. 04–0784), indicating that the branched gold nanocrystals are pure face-centered cubic (fcc) Au crystals.

The crystal orientation and growth direction of the branched gold nanocrystals were studied by low- and high resolution transmission electron microscopy (HRTEM). Fig 2a shows a typical branched structure magnifying image of gold nanocrystals and the inset shows the corresponding selected area electron diffraction (SAED) pattern. The angles between main trunks and side branches are ~68° which are similar to the previous report.[23] In the SAED pattern, the spots with hexagonal symmetry were indexed to the $[\bar{1}10]$ zone axis of cubic gold, which revealed that each branch was a single crystal with (111) lattice planes as the top surface. The 68° is identical to the theoretical angle between two equivalent <331> directions of cubic gold in the $(\bar{1}10)$ projection plane. The HRTEM image of the trunk tip from a single gold branch (shown in Figure 2c) presents clear lattice fringes with d spacing of 0.236 nm, which confirm that the obtained branches of gold nanocrystals are single crystals with a (111) plane and grown along the <331> direction. To our knowledge, such particular crystal growth has not been reported for gold so far. In addition, the associated EDX spectrum presented in Figure 2b shows only the Au signals except the Cu signals arising from the carbon-coated Cu grid used during the HRTEM analysis, confirming the formation of pure Au crystals.
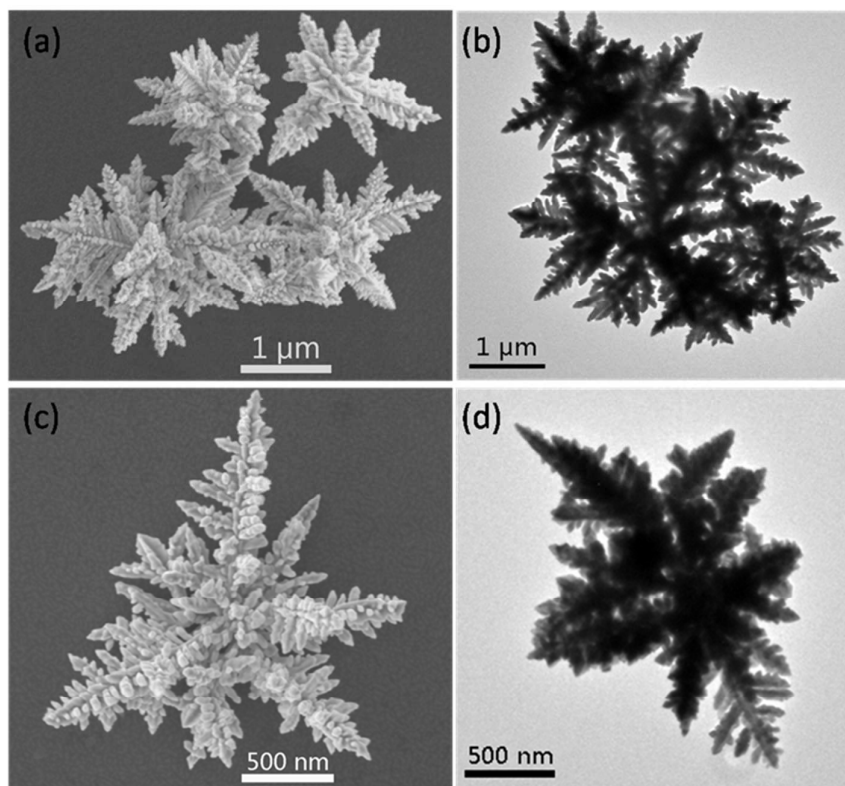
Figure 1. SEM (a, c) and TEM (b, d) images of branched gold nanocrystals obtained in the standard solution, that is, 10 mL mixture solution which contains 0.4 mL $HAuCl_4$ (25 mM), 0.4 mL PDDA, 0.2 mL HCl (1 M), 2 mL AA (50 mM) and 7 mL pure water.
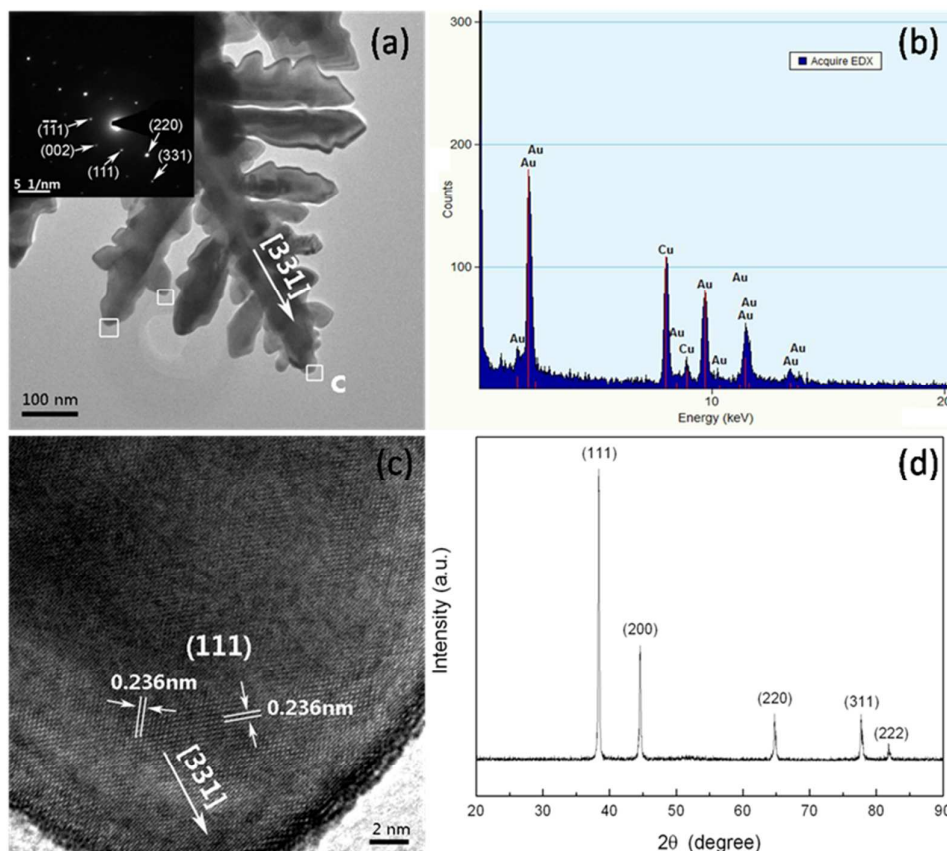

Figure 2. (a) A typical branched structure magnifying image of gold nanocrystals (the inset shows the corresponding SAED pattern). (b) EDX spectrum. (c) HRTEM image of the area marked in (a). (d) XRD pattern of the as-synthesized branched gold nanocrystals obtained under typical conditions.

3.2 Effects of the Concentrations of $HAuCl_4$ and PDDA ([$AuCl_4^-$], [PDDA])

While we have shown SEM and TEM images of branched gold nanocrystals prepared in optimal conditions (i.e., in the standard solution), the formed nanoshapes were very sensitive to the concentrations of $HAuCl_4$ and PDDA. To produce the typical branched gold nanocrystals, the optimum ratio between $HAuCl_4$ and PDDA is 1:50. However, appropriate concentrations of $HAuCl_4$ and PDDA were also necessary, higher or lower were both undesirable for the controllable synthesis of ideal branched nanocrystals. A comparative study was firstly conducted by changing the concentrations of $HAuCl_4$, while the other conditions were kept constant. As shown in Figure 3a, monodispersed polyhedral nanoparticles with size range from 200 to 300 nm were formed when [$AuCl_4^-$] was very low (0.25 mM). When [$AuCl_4^-$] was

increased to 0.5 mM, branched nanoparticles of 250–400 nm (Figure 3b) were formed. Typical well-defined branched nanocrystals were obtained (seen Figure 1) when further adjusting of $[AuCl_4^-]$ to 1mM. Upon continuous increase of $[AuCl_4^-]$ to 2 mM and 3mM, typical branched nanocrystals couldn't be formed, except for some dispersed and disordered nanobranches (Figure 3c, 3d). From this, we deduce that as the source of gold atoms, a lower concentration of $HAuCl_4$ provides less Au^{3+} in the reaction system and thus insufficient to the formation of ideal branched nanostructures. On the other hand, higher $[AuCl_4^-]$ caused the excessive growth and disintegrated typical branched gold nanocrystals into disordered nanobranches.

Furthermore, the influence of [PDDA] on the morphology of branched gold nanocrystals is conspicuous. Individually adjusted the [PDDA], we obtained some evolutions as follows. Firstly, when PDDA was absent, $AuCl_4^-$ ions were quickly reduced to Au atoms, which were then randomly aggregated to form gold nanoparticles with rough surfaces and irregular size distribution (Figure 4a). When [PDDA] was 25 mM, agglomerated nanocrystals (~1μm) without obvious branched structures were obtained (Figure 4b). When [PDDA] was increased to 100 mM, desired branched nanostructures (~3 μm) with more branches were formed (Figure 4c). If continuous increasing of [PDDA] to 200 mM, just small irregular nanocrystals (~1 μm) were presented (Figure 4d), without typical branches appearing, which were similar to Figure 4b. This implies that PDDA serves as a strong shape controller to assist the formation of branched gold nanostructures. Meanwhile, A proper concentration is necessary, too low or too high are both unfavorable for typical branched nanocrystals growth. The detailed function mechanism will be discussed latter.
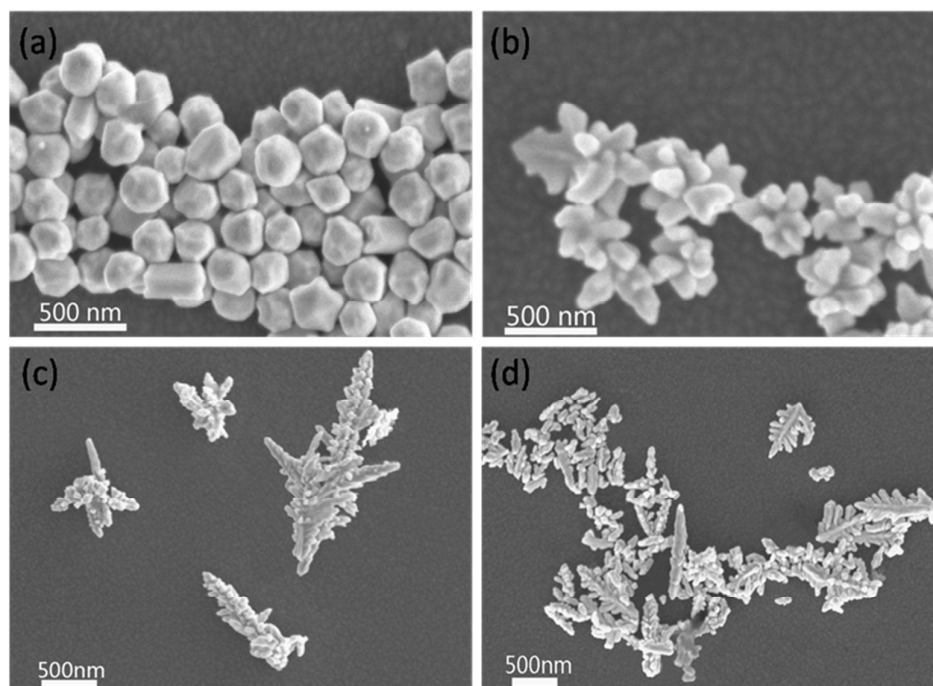
Figure 3. SEM images of products synthesized at 95 °C for 30 min in a pure water solution containing 50 mM PDDA, 20 mM HCl, 10 mM AA and different

concentrations of HAuCl$_4$: (a) 0.25, (b) 0.5, (c) 2 and (d) 3 mM.
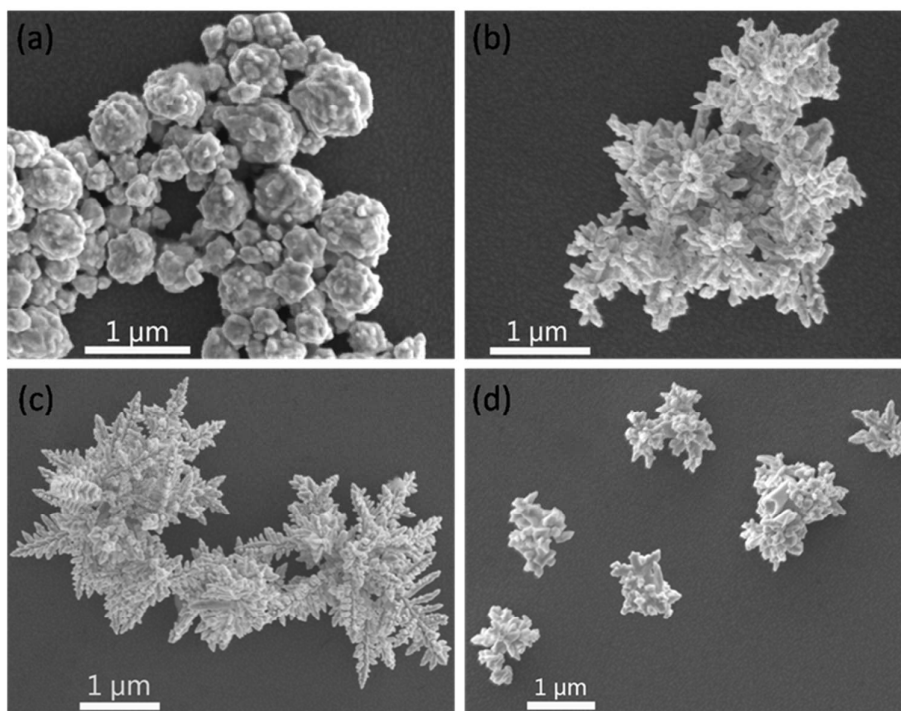
Figure 4. SEM images of products synthesized at 95 $^{\circ}$C for 30 min in a pure water solution containing 1 mM HAuCl$_4$, 20 mM HCl, 10 mM AA and different concentrations of PDDA: (a) 0, (b) 25, (c) 100 and (d) 200 mM.

3.3 Effects of pH Value and Reaction Temperature

We found that the size and shape of branched gold nanocrystals could be further adjusted through introduction of acidic or basic solutions to the initial gold precursor. In this way, various size and shape evolutions of branched gold nanocrystals were presented along with the different pH values of reaction system. Typical branched nanocrystals with average size of 500 nm (Figre 5a) , 1 μm (Figure 5b), 1.5 μm (Figure 5c), 2 μm (Figure 1) were obtained when the concentrations of HCl in the initial gold precursor were 0, 5, 10, 20mM, respectively (the corresponding pH values were 6, 5, 4, 3, respectively). Apparently, the sizes of branched gold nanocrystals were increased, the branches were gradually idealized with the increase of HCl concentration at this time. While, if continuous increasing the concentrations of HCl, an undesirable evolution tendency would be formed. The branches of gold nanocrystals disappeared, but instead, dense bulks with nanoparticles on the surface were formed (Figure 5d) when the HCl concentration was 40 mM (pH=2). Continuously increasing the concentration to 80 mM (pH=1), various irregular nanobulks with size of ~1 μm would be formed, no branched nanocrystals were obtained (Figure 5e). This reflects that the dimensions of branched gold nanocrystals can be tailored effectively when weak acidity were existing, which have been similarly demonstrated in the past research.[27] Differently, high concentration of acid

(pH ≤2) would bring about the disorder (both sizes and shapes) of branched gold nanostructures.

In contrast to the acidic solutions, the evolution could be caused by the addition of basic solutions. We found that a small addition of NaOH expedited the color change of the gold precursor solution and decreased the sizes of the final gold nanocrystals. For example, when 0.1 mL of 1 M NaOH was added to the precursor, the pH value of reaction system was 7, a wine red color was observed within several minutes. In this case, the majority of the final products were 300 nm gold nanospheres with smooth surface (Figure 5f). Larger nano-ellipsoids (~400 nm) with lots of nanoparticles (~20 nm) absorbed on each surfaces were obtained when 30 mM of NaOH was introduced (Figure 5g), the corresponding pH=8. However, when we adjusted the concentration of NaOH to 0.1 M (pH=12), a dark red color was appeared, suggesting the rate of reduction was greatly enhanced. Then, irregular gold nanostructures were produced without clear shapes and sizes (Figure 5h).

These above results suggest that acidity and basicity of reaction solutions can kinetically manipulate the reduction rate of gold ions, and this in turn affects the initial gold nucleation process, which is one of determining factors for the shape and size of the final products. We believe the oxidation of gold atoms[29] occurred in our experiments, relatively weak acidity (pH from 3 to 6) could effectively decrease the oxidation rate of gold atoms and cause the size evolution of typical branched gold nanostructures. While highly acidity would inhibit the reduction of gold ions, the gold nanocrystals tend to a planar growth, then the final disordered gold nanostructures without typical branches were formed. On the contrary, neutral and basic conditions could enhance the reduction of gold ions. Hydrogen ions were consumed by hydroxyl ions and hence smaller gold nanocrystals were produced rapidly when introduction a small amount of NaOH. In addition, the irregular gold nanostructures under strong basicity were caused by the fast and disordered crystal growth of gold nucleis.

Previous work on the morphology-controllable synthesis of gold nanocrystals revealed that an appropriate reaction temperature is essential to obtain the desired product because the reaction temperature greatly affects the reducing power of reductant and the diffusion constant of reaction system.[15, 30-32] Experiments under different reaction temperatures were thus conducted in this study. Pure nanobranches were synthesized in the standard solution without heating process, the reaction temperature was room temperature, 26 °C (Figure 6a). These branched structures comprised main trunks and side branches were almost dispersive, no aggregation between them to form typical hierarchical architecture. In this case, low reaction temperature caused low reducing power of AA, insufficient gold nucleis existing in the reaction system, meanwhile, the diffusion rate of reduction small gold nanoparticles was too slow to ensure the radial growth of these nucleis. Hence, the initial gold nucleis tended to the formation of specific single nanobranches assisted by PDDA. When the temperature was increased to 60 °C, the main products were still nanobranches, exceptionally, hierarchical branched nanostructures with size of ~2 μm appeared. Thus, it can be deduced that higher reaction temperature increased the reducing power of AA so that abundant gold nucleis could be formed and then the

relatively higher diffusion constant would provide a possibility for the three-dimensional growth of these nucleis to form the desired branched gold nanostructures.

In general, to obtain the typical branched gold nanocrystals, ensuring the sufficient reducing power of AA and higher diffusion constant of reaction system were preconditions, relatively slow nucleation and growth of gold nucleis were then indispensable.
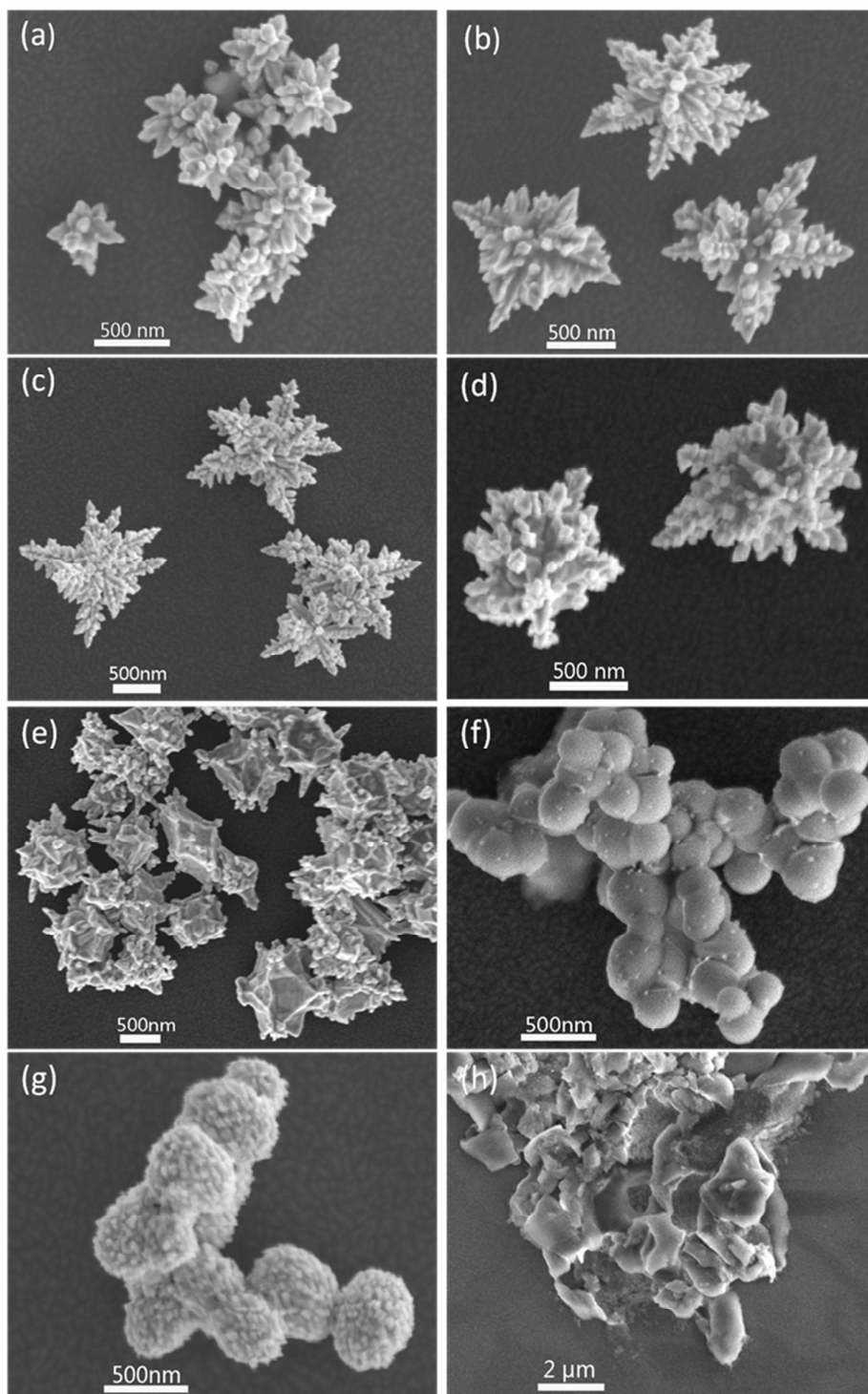
Figure 5. SEM images of gold nanostructures grown at varying pHs: (a) pH=6, (b) pH=5, (c) pH=4, (d) pH=2, (e) pH=1, (f) pH=7, (g) pH=8, (h) pH=12. The corresponding HCl concentrations (a) to (e) were 0, 5, 10, 40 and 80 mM. The corresponding NaOH concentrations (f) to (h) were 10, 30 and 100 mM.
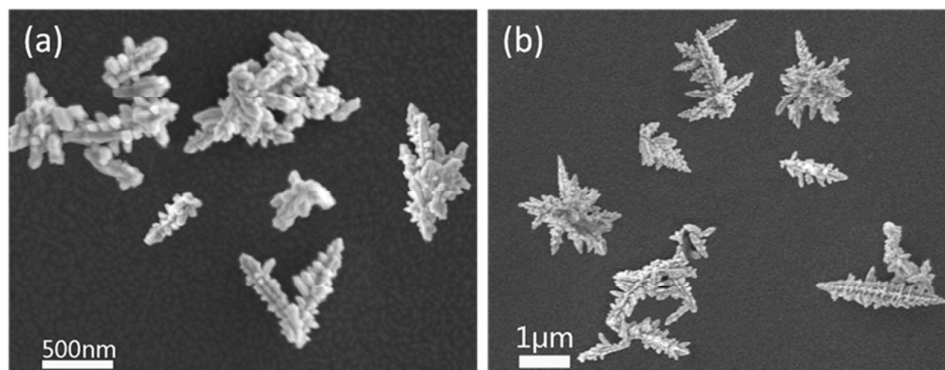
Figure 6. SEM images of products synthesized in the standard solution under different reaction temperatures: (a) T=26 $^{\circ}$C, (b) T=60 $^{\circ}$C

3.4 Formation Mechanism

The formation process is always a focus topic in research on anisotropic gold nanostructures. It has been reported that branched gold nanostructures could be obtained through a nonequilibrium kinetically controlled synthesis process when the driving force is large enough.[33] The kinetic control can be realized by substantially slowing down the precursor decomposition or reduction process.[3] Therefore, the formation of more complicated nanostructures requires a higher driving force, i.e., a lower reduction but higher diffusion constant of reaction system, which is in agreement with our earlier results.

Products formed under different reaction times from 5 s to 2 h were collected to further understand the nucleation and growth process of the typical branched gold nanocrystals, as shown in Figure 7. We found that branched nanoparticles with size of 550—650 nm were formed within 5 s after AA was added (Figure 7a). Actually these branched nanoparticles were the original of typical branched nanostructures, which were grown radially from central particles. However, there were only short main trunks in these branched nanostructures, hardly any side branches or leaves were gown out. These initial trunks were granular or rodlike with smooth surfaces. More side branches were appeared within 30 s (Figure 7b). The sizes (~1 μm) were increased and the branched tips were distinct. Further growth and aggregation made the incomplete branches into the organized assignment with large amount of leaves coupled (Figure 7c) within 1 min. Thus, the basic shapes of typical branched nanocrystals were formed. Panels d and e from Figure 7 shows the nanostructures obtained at 5 and 20 min, respectively. The hierarchical branched nanostructures with compact connectivity were gradually formed and the branches growth continued after

5 min passed. Ideal branched nanocrystals with clear trunks and leaves were obtained after 20 min. The almost symmetrical growth pattern, the size and the completeness of three-dimensional branched structures were both close to the latter typical branched nanocrystals which were obtained within 30 min (Figure 1). It means that the whole nucleation and growth of typical branched nanocrystals lasted for about 20 min. When the reaction was maintained for 2h, the typical structures of branched nanocrystals were stabilized. The whole nanocrystals were branchy and each branch has been fully-grown (Figure 7f).

Such evolution in the branched gold nancrystals geometry was further confirmed from the corresponding absorption spectra in Figure 8. It was found that two principal surface plasmon resonance (SPR) absorption peaks characteristic of the short (transverse band, T-SPR) and long (longitudinal band, L-SPR) axes were normally exhibited to anisotropic gold nanostructures.[34] In our results, the strong absorption at 360−400 nm can be assigned to the T-SPR of each branched tip from gold nanocrystals. The weak band at 650−710 nm is a result of the L-SPR, which is due to the multiple coupling between neighboring main trunks and side branches. Apparently, both T-SPR and L-SPR spectra were red-shift and their intensity gradually increased when the reaction times was from 5 s to 20 min. This indicated that the nucleation and growth of branched nanocrystals were persistently occurring during this time. The size was gradually increasing in theory, which has been demonstrated in Figure 7. Elongating the reaction times to 30 min and 2 h, the absorption peaks were stabilized at 400 nm and 710 nm, the intensity were almost invariable. It suggested that the growth of gold nanostructures tended to be stabilized after 30 min reaction, which was consistent with the SEM observations.

From the above results, we proposed the possible formation process of branched gold nanocrystals. First, surfactant PDDA is known to be a cationic polyelectrolyte and thus an initial strong electrostatic interaction between PDDA and $AuCl_4^-$ ions leads to the formation of stable ion pairs in the precursor complex. When the weak reducing agents, AA, were added, $AuCl_4^-$ were slowly released from the ion pairs and reduced to Au^0. Then the Au^0 would aggregate and form the initial Au nucleis, which were controlled through the selective adsorption of PDDA on the specific Au surfaces.[28] These Au nucleis became the growth centers of branched nanocrystals in the subsequent crystal growth. Meanwhile, continuous reduction created small Au nanoparticles dissolved into the solution. The growth continued as these small particles diffused to and adsorbed on the Au nucleis. Thus, the initial branched nanoparticles were formed. In the second stage, excessive PDDA molecules and weak acidic conditions may provide a delicate balance between nucleation ratio and diffusion ratio for the nonequilibrium, favoring the kinetically controlled process of anisotropic growth. In this case, the specific absorption of PDDA on Au nucleis surfaces could also considerably contribute to the formation of the hierarchical branched gold nanocrystals with the top (111) surface. Specially, PDDA molecules preferentially absorbed on (111) planes of Au nuleis, and consequently the growth rate along the <111> direction was reduced while other directions, especially <331> direction was enhanced. Finally, with the sizes increasing to ~2 μm and the clear

symmetrical branches grown fully, our ideal typical branched gold nanostructures obtained. In this stage, the Ostwald ripening was considered to be the determing factor for adjusting the branched nanostructures. Because the adjustment was a slow thermodynamic process,[26] which lasted for about 19 min. The harmonious growth between large trunks and small branches promoted the orderless branched gold nanostructures to turn into ideal morphology with desired shapes and uniform sizes . In short, we proposed three key factors for the formation: (i) the weak reducing agent (AA) provided a slow reducing rate for the nucleation; (ii) excessive PDDA molecules and relatively weak acidic conditions dominated the crystal growth in the nonequilibrium solutions; (iii) the later adjustment was a slow Ostwald ripening process dominated by thermodynamics.

In addition, the as-prepared branched gold nanocrystals were very stable for months due to the electrostatic repulsion and steric stabilization provided by cationic surfactant PDDA.
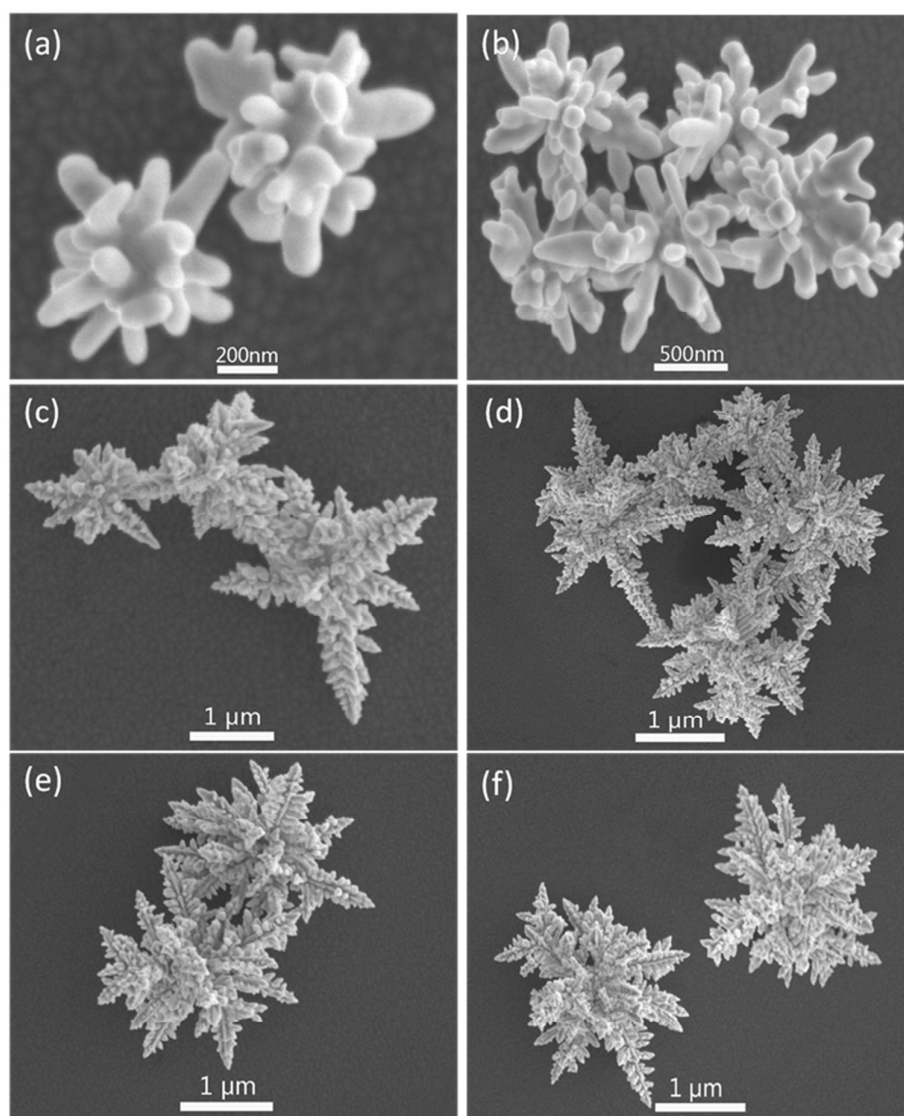
Figure 7. SEM images of branched gold nanocrystals obtained in the standard solution under different reaction times: (a) 5 s, (b) 30 s, (c) 1 min, (d) 5 min, (e) 20 min and (f) 2 h.
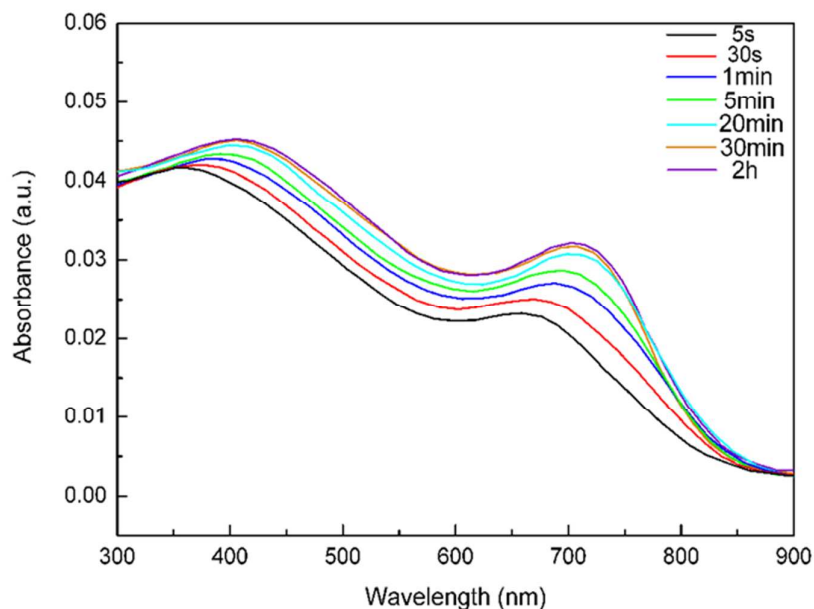
Figure 8. UV-Vis absorption spectra of the standard solution recorded at several reaction times.

4. Conclusions

In summary, we report a facile approach for controllable synthesis of branched gold nanocrystals in acidic aqueous solution assisted by cationic surfactant PDDA. These branched gold nanocrystals (~2 μm) with a single crystalline, three-dimensional hierarchical structure were comprised of main trunks and almost symmetrical side branches. Radial growth from central particles was unique, which finally facilitated the branched gold nanocrystals to present a [111] top surface and grown along <331> direction. The effects of the experimental parameters on the morphology of gold nanocrystals have been discussed in some detail. Several major results are as follows: (1) a proper concentration, ratio between $HAuCl_4$ and PDDA was found to be crucial for the formation of typical branched gold nanocrystals, since $HAuCl_4$ was the source of gold atoms and PDDA acted as shape-directing agents by selectively absorption on the specific Au crystal surface; (2) the dimension of branched gold nanocrystals could be tailored by introducing a given amount of acidic and basic solution to the initial gold precursor; (3) to obtain the typical branched gold nanocrystals, ensuring the sufficient reducing power of weak reducing agent (AA) and higher diffusion constant of reaction system were preconditions, relatively slow nucleation and growth of gold

nucleis were then indispensable.

A possible three-staged formation mechanism of initial branched nucleation, subsequent branched nanostructures growth and the final morphology adjustment was proposed on the basis of reaction times and corresponding absorption spectra. Additionaly, these unique anisotropic nanostructures with broad absorption range and their size-dependent red-shift suggest the potential optical, SERS and surface plasmonic, etc., applications of the obtained branched gold nanocrystals. Further study will focus on these potential applications.

Acknowledgments

Notes and References

1   P. Zijlstra, J. W. M. Chon and M. Gu, *Nature*, 2009, **459**, 410-413.
2   Y. Mikami, A. Dhakshinamoorthy, M. Alvaro and H. Garcia, *Catal. Sci.Technol.*, 2013, **3**, 58−69.
3   Y. Xia, Y. Xiong, B. Lim and S. E. Skrabalak, *Angew. Chem., Int. Ed.*, 2009, **48**, 60-103.
4   Z. Wang and Y. Lu, *J. Mater. Chem.*, 2009, **19**, 1788-1798.
5   X. Huang, I. H. El-Sayed, W. Qian, M and A. El-Sayed, *J. Am. Chem. Soc.*, 2006, **128**, 2115-2120.
6   K. L. Cheung, H. J. Chen, Q. L. Chen, J. F. Wang, H. P. Ho, C. K. Wong and S. K. Kong, *Nanoscale*, 2012, **4**, 4447-4449.
7   M. Grzelczak, J. Perez-Juste, P. Mulvaney and L. M. Liz-Marzan, *Chem. Soc. Rev.*, 2008, **37**, 1783-1791.
8   T. K. Sau and A. L. Rogach, *Adv. Mater.*, 2010, **22**, 1781-1804.
9   H. Y. Liu and Q. Yang, *CrystEngComm*, 2011, **13**, 2281-2288.
10 Y. N. Wang, W. T. Wei, C. W. Yang and M. H. Huang, *Langmuir*, 2013, **29**, 10491-10497.
11 T. K. Sau and C. J. Murphy, *J. Am. Chem. Soc.*, 2004, **126**, 8648-8649.
12 D. Seo, C. I. Yoo, J. C. Park, S. M. Park, S. Ryu and H. Song, *Angew. Chem., Int. Ed.*, 2008, **47**, 763-767.
13 L. Wang, C. H. Liu, Y. Nemoto, N. Fukata, C. W. Wu and Y. Yamauchi, *RSC. Adv.*, 2012, **2**, 4608-4611.
14 G. Maiorano, L. Rizzello, M. A. Malvindi, S. S. Shankar, L. Martiradonna, A. Falqui, R. Cingolani and P. P. PomPa, *Nanoscale*, 2011, **3**, 2227-2232.

15   D. Y. Kim, T. Yu, E. C. Cho, Y. Ma, O. O. Park and Y. Xia, *Angew. Chem., Int. Ed.*, 2011, **50**, 6328-6331.

16   L. Wang, M. Imura and Y. Yamauchi, *CrystEngComm*, 2012, **14**, 7594-7599.

17   H. Liu, Y. Xu, Y. Qin, W. Sanderson, D. Crowley, C. H. Turner and Y. Bao, *J. Phys. Chem. C*, 2013, **117**, 17143-17150.

18   M. Pan, H. Sun, J. W. Lim, S. R. Bakaul, Y. Zeng, S. Xing, T. Wu, Q. Yan and H. Chen, *Chem. Commun.*, 2012, **48**, 1440-1442.

19   D. P. Huang, Y. Y. Qi, X. T. Bai, L. J. Shi, H. Jia, D. J. Zhang and L. Q. Zheng, *ACS Appl. Mater. Interfaces*, 2012, **4**, 4665–4671.

20   J. P. Xie, Q. B. Zhang, J. Y. Lee and D. I. C. Wang, *ACS Nano*, 2008, **2**, 2473-2480.

21   B. R. Danger, D. Fan, J. P. Vivek and I. J. Burgess, *ACS Nano*, 2012, **6**, 11018-11026.

22   N. Ortiz and S. E. Skrabalak, *Cryst. Growth Des.*, 2011, **11**, 3545-3550.

23   Y. Qin, Y. Song, N. J. Sun, N. N. Zhao, M. X. Li and L. M. Qi, *Chem. Mater.*, 2008, **20**, 3965-3972.

24   M. Pan, S. Xing, T. Sun, W. Zhou, M. Sindoro, H. H. Teo, Q. Yanb and H. Chen, *Chem. Commun.*, 2010, **46**, 7112-7114.

25   T. Huang, F. Meng and L. M. Qi, *Langmuir*, 2010, **26**, 7582-7589.

26   D. P. Huang, X. T. Bai and L. Q. Zheng, *J. Phys. Chem. C*, 2011, **115**, 14641-14647.

27   C. C. Li, L. K. Shuford, M. H. Chen, E. J. Lee and S. O. Cho, *ACS Nano*, 2008, **2**, 1760-1769.

28   C. C. Li, L. Sun, Y. Q. Sun and T. Teranishi, *Chem. Mater.*, 2013, **25**, 2580-2590.

29   C. K. Tsung, X. Kou, Q. Shi, J. Zhang, M. H. Yeung, J. Wang and G. D. Stucky, *J. Am. Chem. Soc.*, 2006, **128**, 5353.

30   B. V. Broek, N. Devoogdt, A. D. Hollander, H. L. Gijs, K. Jans, L. Lagage, S. Muyldermans, G. Maes and G. Borghs, *ACS Nano*, 2011, **5**, 4319-4328.

31   Y. Huang, W. Wang, H. Liang and H. Xu, *Cryst. Growth Des.*, 2009, **9**, 858-862.

32   S. Trigari, A. Rindi, G. Margheri, S. Sottini, G. Dellepiane and E. Giorgetti, *J. Mater. Chem.*, 2011, **21**, 6531-6540.

33   J. Xiao and L. Qi, *Nanoscale*, 2011, **3**, 1383-1396.

34   X. Xu and M. B. Cortie, *Adv. Funct. Mater.*, 2006, **16**, 2170-2176.